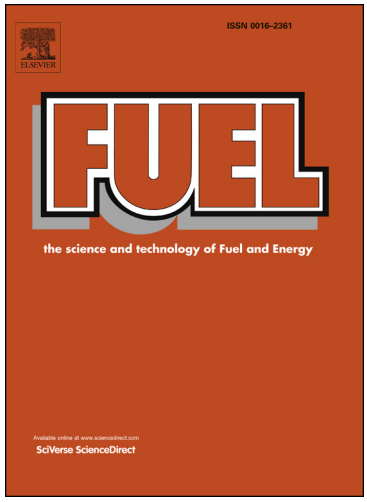

Full Length Article

Two-stage Lagrangian modeling of ignition processes in ignition quality tester and constant volume combustion chambers

Adamu Alfazazi, Olawole Abiola Kuti, Nimal Naser, Suk Ho Chung, S. Mani Sarathy

PII: S0016-2361(16)30754-2
DOI: http://dx.doi.org/10.1016/j.fuel.2016.08.017
Reference: JFUE 10824

To appear in: *Fuel*

Received Date: 1 January 2016
Revised Date: 20 July 2016
Accepted Date: 1 August 2016

Please cite this article as: Alfazazi, A., Abiola Kuti, O., Naser, N., Ho Chung, S., Mani Sarathy, S., Two-stage Lagrangian modeling of ignition processes in ignition quality tester and constant volume combustion chambers, *Fuel* (2016), doi: http://dx.doi.org/10.1016/j.fuel.2016.08.017

Two-stage Lagrangian modeling of ignition processes in ignition quality tester and constant volume combustion chambers

* Adamu Alfazazi [a]
Adamu.Fazazi@kaust.edu.sa

Olawole Abiola Kuti [b]
olawole.kuti@city.ac.uk

Nimal Naser [a]
nimal.naser@kaust.edu.sa

Suk Ho Chung [a]
SukHo.Chung@kaust.edu.sa

* S. Mani Sarathy [a]
mani.sarathy@kaust.edu.sa

[a] King Abdullah University of Science and Technology (KAUST), Clean Combustion Research Center (CCRC), Thuwal 23955-6900, Saudi Arabia

[b] Department of Mechanical Engineering & Aeronautics, School of Engineering & Mathematical Sciences City University London, Northampton Square EC1V 0HB, London UK

*Corresponding Author
Tel. No.: +966548018357
Combustion and Pyrolysis Chemistry Laboratory
Clean Combustion Research Center
King Abdullah University of Science and Technology
Thuwal, Saudi Arabia

ABSTRACT

The ignition characteristics of *iso*-octane and *n*-heptane in an ignition quality tester (IQT) were simulated using a two-stage Lagrangian (TSL) model, which is a zero-dimensional (0-D) reactor network method. The TSL model was also used to simulate the ignition delay of *n*-dodecane and *n*-heptane in a constant volume combustion chamber (CVCC), which are archived in the engine combustion network (ECN) library (http://www.ca.sandia.gov/ecn). A detailed chemical kinetic model for gasoline surrogates from the Lawrence Livermore National Laboratory (LLNL) was utilized for the simulation of *n*-heptane and *iso*-octane. Additional simulations were performed using an optimized gasoline surrogate mechanism from RWTH Aachen University. Validations of the simulated data were also performed with experimental results from an IQT at KAUST. For simulation of *n*-dodecane in the CVCC, two *n*-dodecane kinetic models from the literature were utilized. The primary aim of this study is to test the ability of TSL to replicate ignition timings in the IQT and the CVCC. The agreement between the model and the experiment is acceptable except for *iso*-octane in the IQT and *n*-heptane and *n*-dodecane in the CVCC. The ability of the simulations to replicate observable trends in ignition delay times with regard to changes in ambient temperature and pressure allows the model to provide insights into the reactions contributing towards ignition. Thus, the TSL model was further employed to investigate the physical and chemical processes responsible for controlling the overall ignition under various conditions. The effects of exothermicity, ambient pressure, and ambient oxygen concentration on first stage ignition were also studied. Increasing ambient pressure and oxygen concentration was found to shorten the overall ignition delay time, but does not affect the timing of the first stage ignition. Additionally, the temperature at the end of the first stage ignition was found to increase at higher ambient pressure and oxygen concentration. Sensitivity analysis was performed using the TSL model to elucidate the reactions that control the overall ignition process. The present TSL modeling approach demonstrates the suitability of using detailed chemical kinetic models to provide insights into spray combustion processes.

Keywords: two-stage Lagrangian model (TSL); ignition quality tester (IQT); constant volume combustion chamber (CVCC), *iso*-octane; *n*-heptane; *n*-dodecane; second stage ignition delay time; first stage ignition delay time.

1.0 INTRODUCTION

An enhanced understanding of physical and chemical processes occurring during autoignition is paramount to the development of advanced combustion engine technologies and future fuels. Such engines include homogeneous charge compression ignition (HCCI) engines and low-temperature combustion (LTC) engines. Combustion processes in these engines are shown to be dominated by the kinetics of intermediate and low-temperature ignition [1]. Autoignition is related to the increase in the rate of chain branching reactions that can drive a combustion system to completion in a short period. More knowledge on this phenomenon is useful for enhancing the performance of the engine, reducing NOx and CO_2 emissions, and improving fuel economy. Such knowledge can be achieved by the development and application of simulation tools with accurate chemical kinetic models.

The development of reliable chemical kinetic models for autoignition relies on well-defined experiments for validation. These include experiments in homogeneous systems such shock tubes [2-4], rapid compression machines [5-10], and the jet stirred reactors [11]. These systems are however mostly limited to gas phase studies. Heterogeneous combustion facilities such as ignition quality tester (IQT) offer an alternative where ignition properties of liquid sprays could be explored. An IQT is a constant volume combustion chamber with a spray injection system. It is designed to measure the ignition delay time of various fuels including low volatility fuels [12]. The temperature, pressure, the mass of fuel injected and charge oxygen concentration in an IQT can be well controlled, which makes an IQT a useful system for producing experimental data for the validation of chemical kinetic models, provided that appropriate simulation tools are available. As reported in [12], a small fuel mass requirement in an IQT makes it an exemplary system to study ignition delay times of fuels that are not readily available in large quantity. Another experimental facility used in generating data for development of chemical kinetic models and

computational fluid dynamic (CFD) simulations is a constant volume combustion chamber (CVCC) [13-17]. This is a high-pressure facility used for generating data for the Engine Combustion Network (ECN) [18-20], a library containing diesel spray experiments at various engine-relevant operating conditions.

In practical combustion systems, ignition delay time is the time difference between the start of injection (SOI) to the start of combustion (SOC). It consists of a physical ignition delay (atomization, vaporization and mixing of fuel and air) and a chemical ignition delay. The chemical ignition delay period of the overall ignition delay occur once the gaseous fuel/air mixture with a suitable temperature and mixture ratio is obtained, such that fast chemical reactions can be initiated [21, 22]. The ignition delay in an IQT and a CVCC comprises of both physical and chemical ignition delay periods. Therefore, it is required for a modeling code to encompass both mixing as well as chemical kinetics for it to be used to predict accurately the ignition processes in these facilities. The two-stage Lagrangian model (TSL) employed in this study describes mixing as a two-stage process that is seen in a frame moving downstream with the normal fluid motion. The model is capable of adopting detailed chemical kinetics while also simulating basic mixing process that are important in turbulent gaseous-jet diffusion flames [18, 19, 22-26].

Only few studies were so far reported using the TSL model. These include the works of Pickett et al. [24], Broadwell et al. [25], and Han et al. [26]. Though these studies provided insight into how the TSL works, they however based their focus on soot and NO_x emission without particular emphasis on ignition. Using the TSL, Meijer et al. [19] studied the effects of mixing on ignition delay time of a diesel fuel surrogate in a constant volume combustion chamber. They found out that as a result of overmixing, the second stage ignition delay time of diesel fuel increases as the injection pressure increase from 1000 to 2000 bar, while the trend of first stage ignition shows the opposite. Cung et al. [27] studied the effect of temperature on ignition delay time of DME in a high-pressure facility using the TSL model. The present study would be among the few of its kind to use the TSL model to investigate, in detail, factors controlling ignition processes. In this study, the ignition delay times of *iso*-octane and *n*-heptane in an IQT were investigated. Also, the model was used to simulate CVCC ignition delay data of *n*-dodecane and *n*-heptane available in

the ECN library [20]. The study of *iso*-octane and *n*-heptane ignition delay time is especially important because these are primary reference fuels (PRF) for octane ratings. *n*-Heptane and *n*-dodecane are used as diesel fuel surrogates [28-30].

The ignition properties of *iso*-octane were previously investigated in shock tubes and RCMs in [9, 30, 31]. However, very little effort was made to study ignition properties of *iso*-octane in IQTs. Similarly, the ignition characteristics of *n*-heptane fuel were extensively investigated in RCMs and shock tubes in [4, 10, 28, 31]. *n*-Heptane ignition has been investigated experimentally and numerically in an IQT by Bogin et al. [32-34]. Key to the outcome of their study is the exhibition of negative temperature coefficient (NTC) behavior by alkanes, including C7 isomers. They also observed the two-stage behavior of alkanes in the NTC region. Dodecane ignition properties using CVCC facilities were also reported in [35-37]. Most of numerical studies on ignition in IQTs or CVCCs adopted reduced chemical kinetic models. Alternatively, the simpler TSL modeling tool can accommodate high-fidelity detailed kinetic models at a reduced computational cost in studying the ignition properties of these fuels in an IQT and CVCC. This work is aimed at testing the ability of the TSL model to reproduce trends in ignition delay time of *iso*-octane and *n*-heptane in an IQT and *n*-heptane and *n*-dodecane in the CVCCs. This study aims to shed more light on ignition properties various fuels and the conditions under which TSL model can be applied. Furthermore, the study is aimed at investigating the physical and chemical processes affecting the ignition delay time of *iso*-octane fuel under IQT conditions. Concerning IQT study, simulations were validated using experimental data from the KAUST research ignition quality tester (KR-IQT) [38], while, for the CVCC, validations were performed using archived ECN data [20] at various charge temperatures and pressures.

2.0 METHODOLOGY:

2.1 TSL model

The two-stage Lagrangian model was used for a zero dimensional (0-D) simulation of *iso*-octane, *n*-heptane and *n*-dodecane spray combustion processes. This is a FORTRAN based code that calculates the species mass fractions, reaction rates, and temperature in a non-premixed turbulent jet. The TSL model,

unlike other 0-D modeling tools, was introduced to preserve the ability to use detailed chemical kinetic models, while also simulating basic mixing process important in turbulent gaseous-jet diffusion flames [23]. Unlike multidimensional CFD modeling approaches that rely on reduced reaction mechanisms with less number of reactions and species, the TSL model has the capability of using a detailed reaction mechanism with little computational cost. Figure 1 gives an explanation of the model.

The model is based on the experimental observation that reactions in gaseous jets occur in two sheets; reactions are initiated in the diffusion regions and continue in regions that are almost homogeneous as a result of turbulent mixing. Entrained hot air from the ambient mixes with the jet fluid in a stoichiometric amount at the flame sheet of the diffusion region, and then, products from the flame sheet region move to the homogeneous core reactor where they mixed homogenously with the incoming fuel jet. This procedure is continued to the flame tip where the remaining fuel is consumed [23-25].

The TSL model typically incorporates two reactors; the first reactor represents the homogeneous regions while the second reactor represents the diffusion flame sheet. The homogeneous regions are represented by a perfectly stirred reactor (PSR), while the diffusion sheets can be modeled as either a 1-dimensional strained diffusion flame or a PSR. Previous studies have shown that the use of the two-reactor PSR model gives similar results as the reactor-flame version at a reduced computational cost [23, 25]. Therefore, in this study, both the homogeneous and the flame sheet regions were modeled as PSRs.

The equations for the conservation of mass and energy which describes the flow field for the homogeneous reactor (modeled as a PSR) is as follows [23, 25]:

$$\frac{dm_h}{dx} = f(x) \tag{1}$$

$$\frac{dY_{k,h}}{dx} = \frac{(1+B)}{m_h}\frac{dm_h}{dx}(Y_{k,f} - Y_{k,h}) + (\frac{\dot{\omega}_k W_k}{\rho})_h \frac{1}{u} \quad k = 1, \dots, K \tag{2}$$

$$\frac{dT_h}{dx} = \frac{(1+B)}{m_h C_p}\frac{dm_h}{dx}\sum_k Y_{k,f}\left(h_{k,f} - h_{k,h}\right) - \frac{1}{\rho_f u C_p} + \sum_k (h_k \dot{\omega}_k W_k)_h - \frac{\dot{q}}{u C_p} \tag{2}$$

$$B = \frac{(f_{st} - f_\infty)}{(|f_h - f_{st}| + \varepsilon)} \tag{3}$$

$$f = \sum_{k=1}^{k} \frac{Y_k}{W_k} \sum_{j=C,H} a_{j,k} M_j \quad (4)$$

The conservation equations for the flame-sheet reactor (modeled as a PSR):

$$1\tau Yk,\infty - Yk,f + BYk,h - Yk,f + (\acute{\omega}kWk\rho)f \quad k=1,\ldots, K \quad (5)$$

$$1\tau CpkYk,\infty hk,\infty - hk,f + BkYk,hhk,h - hk,f - 1\rho fCpk(hk\acute{\omega}kWk)f - qCp \quad (6)$$

Where x is axial distance from the nozzle; $m=\rho uA$ is the axial mass flow rate. The first equation for the homogeneous reactor requires a function $f(x)$, which provides the entrainment rate of a surrounding fluid into the jet.

The benefit of using the TSL model, apart from its capability to use large kinetic mechanism in less computational expenses, is that preparation of the tool and its input is easier than CFD codes. Inputs required by the model include state variables of the jet (temperature, pressure, composition); illustration of the jet (nozzle hole diameter, velocity), and parameters that control entrainment. The TSL model uses CHEMKIN, TWOPNT and DASSL subroutines. The CHEMKIN program evaluates chemical production rates and writes a linking file, and then DASSL integrates the first-order differential equations for the reactors while TWOPNT solves the numerical solution to finite differential equations. An executable (TSL.exe) reads the CHEMKIN linking file and the input files together with the boundary conditions and writes both text and binary output files [24]. Details of the formulation and description of TSL can be found in previous works [22-26].

2.2 Approach

Two conditions can be studied using the TSL model: transient ignition and steady-state flame combustion. The focus of the present work is on ignition, so the flame-sheet reactor was turned off by maintaining its temperature at 350 K. The homogeneous reactor ignites allowing the analyses of mixing effects on ignition delay. In running this code, both detailed and reduced chemical kinetic models were employed. For *iso*-octane and *n*-heptane, a comprehensive gasoline surrogate mechanism from LLNL [39] with 1858 chemical species and 7809 elementary reactions was utilized. Additionally, an optimized chemical

kinetics model from RWTH Aachen University for gasoline surrogates [40] consisting 335 chemical species and 1610 elementary reactions was used for validation of *iso*-octane in the IQT. For *n*-dodecane, detailed and reduced kinetic models by Sarathy et al. [41] and Narayanaswamy [37] were respectively utilized.

As earlier stated, validations of the simulated data were performed against previous experimental results using the IQT [38] and CVCC [20]. The experimental conditions used for this simulation are presented in Table 1.

The TSL code is only capable of handling simulations in gas phase, thus the liquid fuel in this study have to be modified to a gas phase condition. Thus, the fuel temperatures were reduced to 230K and 300K for IQT and CVCC simulations, respectively. This is to ensure that the adiabatic flame temperature of the gas jet matches the adiabatic flame temperature of the liquid fuel. Again, for the gas to have the same mass flow and momentum as the liquid fuel, the density of the liquid was reduced and the diameter of the orifice was enlarged. Details on the calculation methods are available in [24].

The rate of mixing into the two reactors is determined by stoichiometric requirement of flame-sheet reactor and also by empirical correlation for jet mixing as proposed by [24]:

$$\frac{m}{m_o} = C\,\frac{x}{d_o}\left(\frac{\rho_a}{\rho_o}\right)^{1/2} \tag{7}$$

where C is a constant (0.32 is for un-reacting jets. For reacting jets, heat release inhibits the air entrainment rate, thus reducing C to 0.16 for momentum driven flames). Subsequently, C of 0.16 is used in these simulations. For more details on simulation method using TSL, please refer to [24].

In engines, ignition delay is the time difference between the start of injection (SOI) to the start of combustion (SOC) [21, 22]. The ignition of typical alkane fuels having NTC behavior is governed by three distinct regimes: first-stage ignition, NTC regime and second-stage ignition. It is important to investigate the processes that influence these regimes of ignition. In the current study, the overall ignition

delay time is taken as the time from the beginning of simulation to the time when the rate of change of temperature with time is maximum $(dT/dt)_{max}$.

3.0 RESULTS AND DISCUSSION

This section consists of four parts. Firstly, the model is compared against experimental data. Next, concentration time-histories, OH rate of production, and sensitivity analysis of selected species are presented. Finally, the effects of injection parameters on first- and second-stage ignition regimes are investigated in detail.

3.1 Validation of ignition delay time

Three different ambient pressures were simulated for the IQT experiments, and the ignition delay time was plotted against various injection temperatures (Fig. 2a) using chemical kinetic models from Mehl et al. [39] and Cai et al. [40]. Similarly, a detailed mechanism by Mehl et al. [39] was used for the simulation of *n*-heptane in the IQT (Fig. 2b).

Results from various chemical kinetic models for *n*-heptane and *n*-dodecane in the CVCC are presented in Fig. 2c. As mentioned previously, *n*-dodecane was simulated using detailed kinetic models by Sarathy et al. [41] and Narayanaswamy et al. [37], while *n*-heptane was simulated using the model by Mehl et al. [39]. Also, the updated mechanism by Cai et al. [40] was utilized to simulate the ECN's *n*-heptane data.

For *iso*-octane, the trends are well captured by the TSL model showing that the ignition delay time decreases with increasing ambient pressure and temperature. The quantitative agreement is also acceptable for *iso*-octane in the IQT and *n*-heptane and *n*-dodecane in the CVCC. iso-Octane simulations using the Cai et.al model [40] show a better agreement with experiments, however quantitative discrepancies of up to 50% still exist. Detailed chemical kinetic models for highly branched hydrocarbons [42-44], such as iso-octane, are not as predictive as those for n-alkanes when attempting to predict even fundamental combustion data such as homogenous ignition delay times in shock tubes. Research is currently underway in KAUST to improve the iso-octane detailed kinetic model, and validate it against experimental data from idealized zero-dimensional reactor experiments.

As presented in Fig. 2b, the simulated IQT *n*-heptane ignition delay qualitatively agrees with the experimental trend, however there is a quantitative over-prediction of the experimental data. The discrepancy in *n*-heptane IQT simulations is partly due to its short ignition delay, which is controlled by physical such as droplet formation and eventual fuel-air mixing. As noted by Bogin et al. [12, 32-34], when ignition delay time is short (< 20 ms), physical processes related to spray break up and vaporization dominate over chemical kinetics. However, when the ignition delay period is long, chemical kinetics plays an important role, as is the case for *iso*-octane. The *n*-heptane CVCC operating conditions enable the system to quickly reach conditions controlled by gas-phase chemical kinetics due to higher injection pressure and smaller nozzle hole diameter. Hence, the time scale between the physical and chemical processes is decreased in the CVCC due to enhanced vaporization and mixing, such that gas-phase chemistry is rate controlling. Therefore, the TSL simulations accurately capture the ignition delay times in the CVCC for both *n*-heptane and *n*-dodecane, especially at higher temperatures. At the lowest temperatures in the CVCC, the model over-predicts the ignition delay time data for n-heptane and n-dodecane. Detailed chemical kinetic models for n-alkanes are not rigorously tested at high pressures and low temperatures due to the lack of experimental data under such conditions. Recent work by Wang and Sarathy [45] has shown an extended low temperature oxidation mechanism involving third O_2 addition reactions accelerates the reactivity of alkanes at low temperatures and high pressures. Including these reactions in detailed kinetic models for n-heptane and n-dodecane may improve the TSL model's ability to predict IQT and CVCC data. Additionally, higher fidelity CFD simulations, such as those and Bogin et al., may improve predictions of IQT, but that is beyond the scope of the present work. It can be noted that the present TSL simluations for n-dodecane agree with experimental data nearly as well as high-fidelity CFD simulations for ECN sprays [18, 46-48].

Figure 2a also shows that at a particular ambient temperature, an increase in ambient pressure shortens the ignition delay time. Similar observation was made by Kobori et al. [49], who explained that ignition delay

time is inversely proportional to the ambient pressure, suggesting that the reactivity of diesel fuel spray is controlled by molar concentration of oxygen. At higher pressures, there is a rise in the oxygen concentration, and this increases the reactivity of the fuel and decreases its ignition delay time.

3.2.1 Mass fraction and rate of production analysis

To gain insight into the chemical kinetics of the two-stage ignition behavior of *iso*-octane, the rate of production (ROP) of OH and mass fraction analyses of some selected species are presented in the supplementary material. Selection of species was based on reactions that have the highest ROPs at the 1st and 2nd stage ignition delay time. For the ROP analysis, positive and negative values mean production and consumption of OH radicals, respectively. The temperature profiles show a well-defined two-stage ignition. The first rise occurs at around 39 ms while reactivity is then suppressed due to NTC reactions. After a brief period, at around 50 ms, the temperature rises again very sharply causing the second-stage ignition.

Formaldehyde could be used as a marker of low temperature chemistry. For this reason, the mass fraction of formaldehyde is plotted against temperature on Fig. 3 of supplementary material. Accumulation of CH_2O starts around 700 K. The mass fraction of CH_2O decreases as the ambient pressure is lowered. Therefore, as noted by [29], since this specie is easily accessible using LIF-optical diagnostics, it could be used as an indicator of an initially fuel-rich premixed reaction region.

The effect of ambient pressure could be seen by fixing the ambient temperature while varying the charge pressure as shown on Fig. 4. It is interesting also to see that the location at which ignitions occur shifts downstream of the nozzle as the ambient temperature and ambient pressure decrease. Lower pressures and lower temperatures result in longer ignition delay times, which allow for more air entrainment downstream and leaner fuel/air mixtures that also decrease reactivity.

3.2.2 Sensitivity analysis

A temperature sensitivity analysis was carried out at 21.27 bar and 750 K at the time of ignition to see the reactions that control the overall oxidation process at the end of NTC (i.e., at second-stage ignition). A rigorous sensitivity analysis is beyond the current capability of the TSL code, so a simple technique was utilized here. Individual reaction rates were doubled and the ignition delay time was recomputed using the TSL code, giving the results in Fig. 5. The percentage sensitivity is defined as. [39]:

$$\%\ sensitivity = \frac{\tau(2ki)-\tau(ki)}{\tau(ki)} * 100 \quad (8)$$

where $\tau(2ki)$ corresponds to ignition delay when the rate coefficient is doubled and $\tau(ki)$ is nominal ignition delay time.

A positive percentage change correlates to longer ignition delay and decrease reactivity while negative percentage change results in shorter ignition delay and increases reactivity. The reaction with the highest negative sensitivity is the most effective in promoting the overall rate of oxidation. H_2O_2 decomposition to 2OH radicals is the most effective in igniting the system.

The sensitivity of H abstraction from the fuel by OH depends on the site from which H is abstracted. H abstractions from *iso*-octane yields negative sensitivities, with the exception of abstraction from the *c*-site carbon atom. The sensitivity analysis shows that H abstraction from *a*-site (a primary carbon) increases the oxidation process greatly because it can abstract 9 H from 3 different sites. On the contrary, OH abstraction from the *c*-site has a positive sensitivity. This is because internal hydrogen abstraction from O_2QOOH to give ketohydroperoxide + OH is curtailed by the fact that abstraction is easier from the carbon bonded to OOH. Since there are no more available H atoms at the *c*-site to be abstracted (see the graph 5b), the reaction scheme cannot produce ketohydroperoxide and OH. This inhibits or slows the low temperature chemistry and delays the final ignition. QOOH decomposition into ketohydroperoxide, OH and subsequent decomposition of ketohydroperoxide into OH also have negative percentage sensitivities. This is because this reaction produces OH and contributes to the early heat release. AC8H18OO-

B4C8ETERAB + OH have positive sensitivity because this reaction is a competing pathway to the low temperature chemistry pathway (i.e. the addition of O_2 to QOOH).

3.3 Effects of ambient oxygen concentration on ignition of *iso*-octane

Reduction in oxygen concentration is mainly achieved through exhaust gas recirculation (EGR) in engines, which are becoming more relevant with the introduction of new engines such as the HCCI or LTC engines. EGR inhibits the formation of NO_x and soot in engines by reducing the flame temperature. However, this is achieved at the expense of increasing emissions of unburned hydrocarbons, and decrease in overall engine cycle efficiency [22, 50]. Also, it is a common practice in IQT experiments to simulate EGR effect by decreasing charge oxygen concentration [33, 34]. This is important for high volatility fuels with short ignition delay times, as it allows the fuel-air mixture to reach pseudo-homogeneous conditions, so that NTC regions become noticeable. To understand the effects of O_2 concentration on ignition delay time, the core temperature was plotted against time in Fig. 6a. Different ambient oxygen concentrations were considered.

Decreasing the oxygen concentration from 22% to 10% increases the ignition delay time. At lower oxygen concentrations, the rate of reaction decreases, as indicated by the dropping of combustion temperature. Less heat is also released at the end of the first stage ignition which leads to an increase in the total ignition delay time at lower oxygen concentration. Additionally, the graph shows that an increase in temperature by 50 K significantly decreases the ignition delay period at all O_2 concentrations. This is due to increase in the overall rate of reaction due to decrease in the activation energy.

Also, in order to have an insight on how oxygen concentration affects ignition location, the core temperature is also plotted against a non-dimensional axial distance in Fig. 6b. As the concentration of oxygen is reduced, the location at which ignition occur shifts further downstream. The ignition location shifts downstream because longer ignition delay times permit more air entrainment, which further reduce reactivity.

3.4 First-stage ignition delay time

The first-stage ignition delay time (τ_f) has a substantial impact on the total ignition delay time (τ_t). As noted by Zhao et al. [51], since τ_t is associated to τ_s (second-stage ignition delay time) through heat release at the end of first stage, then much of the information that is required to study chemical kinetics of ignition is contained in τ_f (first stage ignition delay time). Therefore it is equally important to study the first-stage ignition delay time.

3.4.1 Effect of ambient pressure on first stage ignition

In order to see these effects, the first-stage ignition delays of *iso*-octane are plotted against ambient pressures for three different temperatures (Fig. 7a). The result suggests that there is a small or negligible effect of ambient pressure on first stage ignition delay at these pressure ranges. This suggests that first stage ignition delay is insensitive to changes in ambient pressure at these conditions. Therefore, the majority of the effect of ambient pressure is in τ_s. A similar trend was observed by [51]. They observed that at low pressure and low temperature, the first stage is insensitive to change in ambient pressure.

3.4.2 Effect of exothermicity on first-stage ignition delay

The temperature at the end of the first-stage ignition is plotted against the ambient temperature in Fig. 7b. As the ambient temperature is increased, the temperature at the end of the first-stage ignition also increases, indicating the role of low temperature heat release on the overall ignition delay time. The temperature increase is however less than the initial temperature difference. Furthermore, T_{ef} (temperature at the end of the first stage ignition) is higher at 21.27 bar than it is at 16.4 and 12.9 bar implying that the role of pressure on the overall ignition delay time is primarily to raise the temperature at the end of the first stage ignition (i.e., but not actually changing the first-stage ignition delay time).

3.4.3 Effect of ambient oxygen concentration on first-stage ignition

To see the effects of oxygen concentration on the first-stage ignition delay time, six different ambient oxygen concentrations were considered. The first stage ignition delay is plotted as a function the different ambient oxygen concentrations on Fig. 8a.

The graph shows that the timing of the first-stage ignition is less affected by the changes in O_2 concentration. However, Fig. 8b shows that O_2 concentration plays a greater role in the low temperature heat release. The temperature at the end of the first-stage ignition increases with increasing O_2 concentration, indicating the faster arrival of the second-stage ignition.

3.5 Strain rate on ignition

As described above, ignition processes involve many intermediate species and radicals. The lifetime of these species and radical is highly influenced by the strain rate. In order to see how this strain rate affects ignition delay time of *iso*-octane in the IQT, the second-stage ignition delay time is plotted at various strain rates in Fig. 9a. The strain rate is defined as the ratio of the inlet velocity u_0 to the orifice diameter d_0, which gives the strain rate in terms of (1/s). Therefore, the strain rates here are obtained at various u_0/d and are representative of various spray injection velocities. As the strain rate is increased, the ignition delay period becomes longer. This is especially evident at lower charge temperatures. To see the possible reason for this behavior, the homogeneous core reactor equivalence ratio is plotted at different strain rates in Fig. 9b. The plot shows that as the strain rate is increased, the core equivalence ratio decreases as a result of overmixing, forming leaner mixtures especially at high strain rates and causing the ignition delay time to increase.

4.0 CONCLUSIONS

In this research, the TSL model was used to simulate the ignition characteristics of *iso*-octane and *n*-heptane in the IQT and *n*-heptane and *n*-dodecane in the CVCC. The quantitative agreement between the simulations and the experiments is acceptable, except for *n*-heptane in the IQT. The inability of the TSL model to predict IQT ignition n-heptane was attributed to the model's inability to accurately capture physical processes when they become rate controlling in ignition processes. The model was used to further investigate other properties of *iso*-octane ignition in the IQT.

In summary the results are as follows;

1. The TSL model is efficient in simulating IQT of long ignition delay time fuels. It is also good for CVCC experiments with high injection pressures, where physical processes do not contribute much to the ignition delay time.

2. Increasing ambient pressure decreases the overall ignition delay time, but it does not to affect the timing of the first stage ignition. However, the temperature at the end of the first stage ignition increases with increase in ambient pressure. This accelerates the arrival of the second stage ignition by increasing the low temperature heat release.

3. Decreasing ambient oxygen concentration lengthens the ignition delay time and shifts the ignition location further downstream. Varying the ambient oxygen concentration does not affect the timing of the first stage ignition. The final temperature at the end of the first stage increases with increases in the concentration of oxygen, which advances the arrival of the second stage ignition delay time.

4. OH Rate of production analysis and mass fraction analysis of some species for *iso*-octane fuel at the end of the first stage ignition showed that IC8KETAB is important, and decomposes to supply early energy to the system. ROP at the end of the second stage ignition showed that the decomposition of H_2O_2 into two OH radicals gives the much-needed energy to finally ignite the system.

5. Sensitivity analysis showed that abstraction of H by OH from *a*, *b* and *d* sites increases the reactivity of *iso*-octane fuel, while abstraction from the *c*-site slows reactivity.

6. Ignition delay times increase as the strain rate is increased. This is because, at very high strain rates, the equivalence ratio is greatly reduced due to overmixing, thereby forming lean mixtures with longer ignition delay times.

5.0 ACKNOWLEDGEMENTS

This work was performed by the Clean Combustion Research Center with funding from King Abdullah University of Science and Technology (KAUST) and Saudi Aramco under the FUELCOM program. Research reported in this publication was also supported by competitive research funding from KAUST.

We thank Samah Y. Mohammed and Nour Atef of Combustion and Pyrolysis Chemistry Team at KAUST for their valuable contributions. We appreciate the assistance of Dr. Lyle M. Pickett from Sandia National Laboratory Combustion Research Facility for guidance in TSL modeling.

REFERENCES

[1] C.K. Westbrook, Chemical kinetics of hydrocarbon ignition in practical combustion systems, Proceedings of the Combustion Institute, 28 (2000) 1563-1577.
[2] D.F. Davidson, D.R. Haylett, R.K. Hanson, Development of an aerosol shock tube for kinetic studies of low-vapor-pressure fuels, Combustion and Flame, 155 (2008) 108-117.
[3] H.-P.S. Shen, M.A. Oehlschlaeger, The autoignition of C8H10 aromatics at moderate temperatures and elevated pressures, Combustion and Flame, 156 (2009) 1053-1062.
[4] H.-P.S. Shen, J. Steinberg, J. Vanderover, M.A. Oehlschlaeger, A shock tube study of the ignition of n-heptane, n-decane, n-dodecane, and n-tetradecane at elevated pressures, Energy & Fuels, 23 (2009) 2482-2489.
[5] C. Allen, G. Mittal, C.-J. Sung, E. Toulson, T. Lee, An aerosol rapid compression machine for studying energetic-nanoparticle-enhanced combustion of liquid fuels, Proceedings of the Combustion Institute, 33 (2011) 3367-3374.
[6] D.M. Karwat, S.W. Wagnon, P.D. Teini, M.S. Wooldridge, On the chemical kinetics of n-butanol: ignition and speciation studies, The Journal of Physical Chemistry A, 115 (2011) 4909-4921.
[7] J. Wurmel, J.M. Simmie, H.J. Curran, Studying the chemistry of HCCI in rapid compression machines, International Journal of Vehicle Design, 44 (2007) 84-106.
[8] M.T. Donovan, X. He, B.T. Zigler, T.R. Palmer, M.S. Wooldridge, A. Atreya, Demonstration of a free-piston rapid compression facility for the study of high temperature combustion phenomena, Combustion and Flame, 137 (2004) 351-365.
[9] X. He, B. Zigler, S. Walton, M. Wooldridge, A. Atreya, A rapid compression facility study of OH time histories during iso-octane ignition, Combustion and flame, 145 (2006) 552-570.
[10] R. Minetti, M. Carlier, M. Ribaucour, E. Therssen, L. Sochet, A rapid compression machine investigation of oxidation and auto-ignition of n-heptane: measurements and modeling, Combustion and Flame, 102 (1995) 298-309.
[11] P. Dagaut, D. Voisin, M. Cathonnet, M. Mcguinness, J.M. Simmie, The oxidation of ethylene oxide in a jet-stirred reactor and its ignition in shock waves, Combustion and flame, 106 (1996) 62-68.
[12] G. Bogin, A.M. Dean, M.A. Ratcliff, J. Luecke, B.T. Zigler, Expanding the Experimental Capabilities of the Ignition Quality Tester for Autoigniting Fuels, SAE International Journal of Fuels and Lubricants, 3 (2010) 353-367.
[13] J. Zhang, W. Jing, W.L. Roberts, T. Fang, Soot temperature and KL factor for biodiesel and diesel spray combustion in a constant volume combustion chamber, Applied Energy, 107 (2013) 52-65.
[14] J.-G. Nerva, C.L. Genzale, S. Kook, J.M. García-Oliver, L.M. Pickett, Fundamental spray and combustion measurements of soy methyl-ester biodiesel, International Journal of Engine Research, 14 (2013) 373-390.
[15] J. Zhang, W. Jing, T. Fang, High speed imaging of OH* chemiluminescence and natural luminosity of low temperature diesel spray combustion, Fuel, 99 (2012) 226-234.
[16] S.A. Skeen, J. Manin, L.M. Pickett, Simultaneous formaldehyde PLIF and high-speed schlieren imaging for ignition visualization in high-pressure spray flames, Proceedings of the Combustion Institute, 35 (2015) 3167-3174.
[17] M. Lapuerta, J.J. Hernández, S.M. Sarathy, Effects of methyl substitution on the auto-ignition of C16 alkanes, Combustion and Flame, 164 (2016) 259-269.
[18] Y. Pei, M.J. Davis, L.M. Pickett, S. Som, Engine combustion network (ECN): global sensitivity analysis of Spray A for different combustion vessels, Combustion and Flame, 162 (2015) 2337-2347.
[19] M. Meijer, B. Somers, J. Johnson, J. Naber, S.-Y. Lee, L.M. Malbec, G. Bruneaux, L.M. Pickett, M. Bardi, R. Payri, Engine Combustion Network (ECN): Characterization and comparison of boundary conditions for different combustion vessels, Atomization and Sprays, 22 (2012).

[20] L. Pickett, G. Bruneaux, R. Payri, Engine Combustion Network, in, http://www.ca. sandia.gov/ecn, 2015.
[21] O.A. Kuti, M. Sarathy, K. Nishida, W. Roberts, Numerical Studies of Spray Combustion Processes of Palm Oil Biodiesel and Diesel Fuels using Reduced Chemical Kinetic Mechanisms, SAE Technical Paper, 10.4271/2014-01-1143 (2014).
[22] A. Alfazazi, O. Kuti, S. Sarathy, IGNITION PROCESSES OF PALM OIL BIODIESEL AND DIESEL FUELS USING A TWO STAGE LAGRANGIAN APPROACH, SAE Technical Paper, 10.4271/2015-01-1861 (2015).
[23] A.E. Lutz, J.E. Broadwell, Two-Stage Lagrangian Model for Mixing and Reactions in a Turbulent Jet, in: F.r. GRI-97/0367 (Ed.) Final report GRI-97/0367, 1997, pp. 2-89.
[24] L. Pickett, J. Caton, M. Musculus, A. Lutz, Evaluation of the equivalence ratio-temperature region of diesel soot precursor formation using a two-stage Lagrangian model, International Journal of Engine Research, 7 (2006) 349-370.
[25] J.E. Broadwell, A.E. Lutz, A turbulent jet chemical reaction model: NO x production in jet flames, Combustion and Flame, 114 (1998) 319-335.
[26] D. Han, M. Mungal, V. Zamansky, T. Tyson, Prediction of NO x control by basic and advanced gas reburning using the Two-Stage Lagrangian model, Combustion and flame, 119 (1999) 483-493.
[27] K. Cung, M. Bhagat, A. Zhang, S.-Y. Lee, Numerical Study on Emission Characteristics of High-Pressure Dimethyl Ether (DME) under Different Engine Ambient Conditions, SAE Technical Paper, 10.4271/2013-01-0319 (2013).
[28] H. Curran, P. Gaffuri, W.J. Pitz, C.K. Westbrook, A comprehensive modeling study of n-heptane oxidation, Combustion and flame, 114 (1998) 149-177.
[29] M.P. Musculus, P.C. Miles, L.M. Pickett, Conceptual models for partially premixed low-temperature diesel combustion, Progress in Energy and Combustion Science, 39 (2013) 246-283.
[30] S. Som, D. Longman, Z. Luo, M. Plomer, T. Lu, Three dimensional simulations of diesel sprays using n-dodecane as a surrogate, in: Fall technical meeting of the eastern states section of the combustion institute, 2011.
[31] J.M. Desantes, J.J. López, S. Molina, D. López-Pintor, Design of synthetic EGR and simulation study of the effect of simplified formulations on the ignition delay of isooctane and n-heptane, Energy Conversion and Management, 96 (2015) 521-531.
[32] G.E. Bogin Jr, E. Osecky, J.-Y. Chen, M.A. Ratcliff, J. Luecke, B.T. Zigler, A.M. Dean, Experiments and Computational Fluid Dynamics Modeling Analysis of Large n-Alkane Ignition Kinetics in the Ignition Quality Tester, Energy & Fuels, 28 (2014) 4781-4794.
[33] G.E. Bogin Jr, E. Osecky, M.A. Ratcliff, J. Luecke, X. He, B.T. Zigler, A.M. Dean, Ignition Quality Tester (IQT) Investigation of the Negative Temperature Coefficient Region of Alkane Autoignition, Energy & Fuels, 27 (2013) 1632-1642.
[34] G.E. Bogin Jr, A. DeFilippo, J. Chen, G. Chin, J. Luecke, M.A. Ratcliff, B.T. Zigler, A.M. Dean, Numerical and experimental investigation of n-heptane autoignition in the ignition quality tester (IQT), Energy & Fuels, 25 (2011) 5562-5572.
[35] L.M. Pickett, C.L. Genzale, G. Bruneaux, L.-M. Malbec, L. Hermant, C.A. Christiansen, J. Schramm, Comparison of diesel spray combustion in different high-temperature, high-pressure facilities, SAE International Journal of Engines, 3 (2010) 156-181.
[36] S. Som, G. D'Errico, D. Longman, T. Lucchini, Comparison and Standardization of Numerical Approaches for the Prediction of Non-reacting and Reacting Diesel Sprays, SAE Technical Paper, 10.4271/2012-01-1263 (2012).
[37] K. Narayanaswamy, P. Pepiot, H. Pitsch, A chemical mechanism for low to high temperature oxidation of n-dodecane as a component of transportation fuel surrogates, Combustion and Flame, 161 (2014) 866-884.
[38] S.Y. Yang, N. Naser, J. Cha, S.H. Chung, Effect of temperature, pressure and equivalence ratio on ignition delay in ignition quality tester (IQT): diesel, n-heptane, and iso-octane fuels under low temperature condition, SAE Journal of Fuel and Lubricants SAE 2015-01-9074 (2015).
[39] M. Mehl, W.J. Pitz, C.K. Westbrook, H.J. Curran, Kinetic modeling of gasoline surrogate components and mixtures under engine conditions, Proceedings of the Combustion Institute, 33 (2011) 193-200.
[40] L. Cai, H. Pitsch, Optimized chemical mechanism for combustion of gasoline surrogate fuels, Combustion and Flame, 162 (2015) 1623-1637.

[41] S. Sarathy, C. Westbrook, M. Mehl, W. Pitz, C. Togbe, P. Dagaut, H. Wang, M. Oehlschlaeger, U. Niemann, K. Seshadri, Comprehensive chemical kinetic modeling of the oxidation of 2-methylalkanes from C 7 to C 20, Combustion and flame, 158 (2011) 2338-2357.
[42] S.Y. Mohamed, L. Cai, F. Khaled, C. Banyon, Z. Wang, M.J. Al Rashidi, H. Pitsch, H.J. Curran, A. Farooq, S.M. Sarathy, Modeling Ignition of a Heptane Isomer: Improved Thermodynamics, Reaction Pathways, Kinetics, and Rate Rule Optimizations for 2-Methylhexane, The Journal of Physical Chemistry A, 120 (2016) 2201-2217.
[43] Z. Wang, L. Zhang, K. Moshammer, D.M. Popolan-Vaida, V.S.B. Shankar, A. Lucassen, C. Hemken, C.A. Taatjes, S.R. Leone, K. Kohse-Höinghaus, N. Hansen, P. Dagaut, S.M. Sarathy, Additional chain-branching pathways in the low-temperature oxidation of branched alkanes, Combustion and Flame, 164 (2016) 386-396.
[44] S.M. Sarathy, T. Javed, F. Karsenty, A. Heufer, W. Wang, S. Park, A. Elwardany, A. Farooq, C.K. Westbrook, W.J. Pitz, M.A. Oehlschlaeger, G. Dayma, H.J. Curran, P. Dagaut, A comprehensive combustion chemistry study of 2,5-dimethylhexane, Combustion and Flame, 161 (2014) 1444-1459.
[45] Z. Wang, S.M. Sarathy, Third O2 addition reactions promote the low-temperature auto-ignition of n-alkanes, Combustion and Flame, 165 (2016) 364-372.
[46] Y. Pei, E.R. Hawkes, S. Kook, G.M. Goldin, T. Lu, Modelling n-dodecane spray and combustion with the transported probability density function method, Combustion and Flame, 162 (2015) 2006-2019.
[47] C. Bekdemir, B. Somers, P. de Goey, DNS with detailed and tabulated chemistry of engine relevant igniting systems, Combustion and Flame, 161 (2014) 210-221.
[48] A. Wehrfritz, O. Kaario, V. Vuorinen, B. Somers, Large Eddy Simulation of n-dodecane spray flames using Flamelet Generated Manifolds, Combustion and Flame, 167 (2016) 113-131.
[49] S. Kobori, T. Kamimoto, A. Aradi, A study of ignition delay of diesel fuel sprays, International Journal of Engine Research, 1 (2000) 29-39.
[50] L.M. Pickett, Low flame temperature limits for mixing-controlled diesel combustion, Proceedings of the Combustion Institute, 30 (2005) 2727-2735.
[51] P. Zhao, C.K. Law, The role of global and detailed kinetics in the first-stage ignition delay in NTC-affected phenomena, Combustion and Flame, 160 (2013) 2352-2358.

ABBREVIATIONS

IQT Ignition quality tester

TSL Two-stage Lagrangian

CVCC Constant Volume Combustion Chamber

ECN Engine combustion network

LLNL Lawrence Livermore national laboratory

KAUST King Abdullah University of Science and Technology

CFD Computational fluid dynamic

τ_f first stage ignition delay time

τ_s second stage ignition delay ime

τ_t total ignition delay time

T_{ef} Temperature at the end of first stage ignition delay time

A	Jet cross-sectional area
Y_k	Mass fraction of species k
K	Number of species
h_k	enthalpy of species k
$_k$	species molar production rate
W_k	Molecular weight of species k
ρ	density
ρ_0	jet source density
m	mass flow rate in the jet
m_o	initial jet mass flow rate
c_p	Specific heat (at constant pressure)
q_R	Radiation loss
f	fuel mixture fraction
$a_{j,k}$	number of atoms of element j in species k
M_j	atomic mass of element j
	Number to avoid the singularity where f_h passes stoichiometric
B	is an expression that controls the homogeneous stream entering the flame-sheet reactor

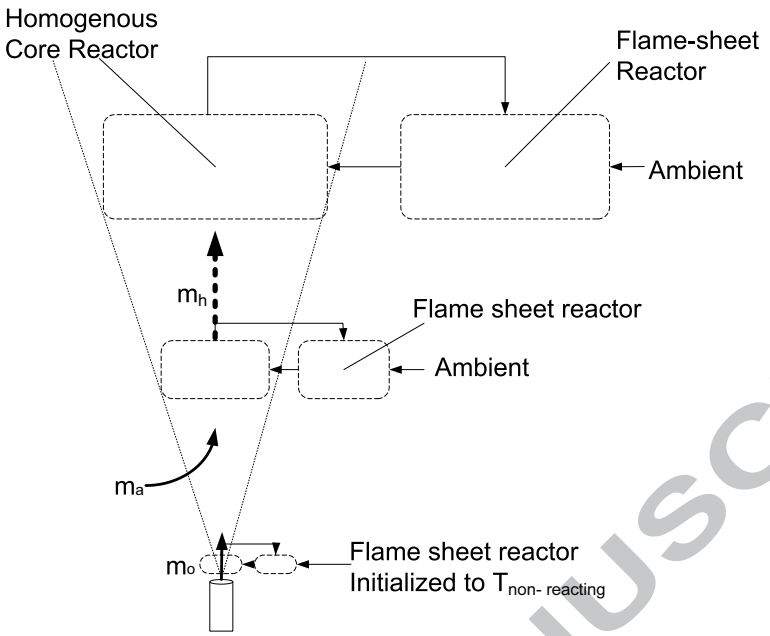

Figure 1. Schematic diagram describing TSL model for turbulent jets [24]

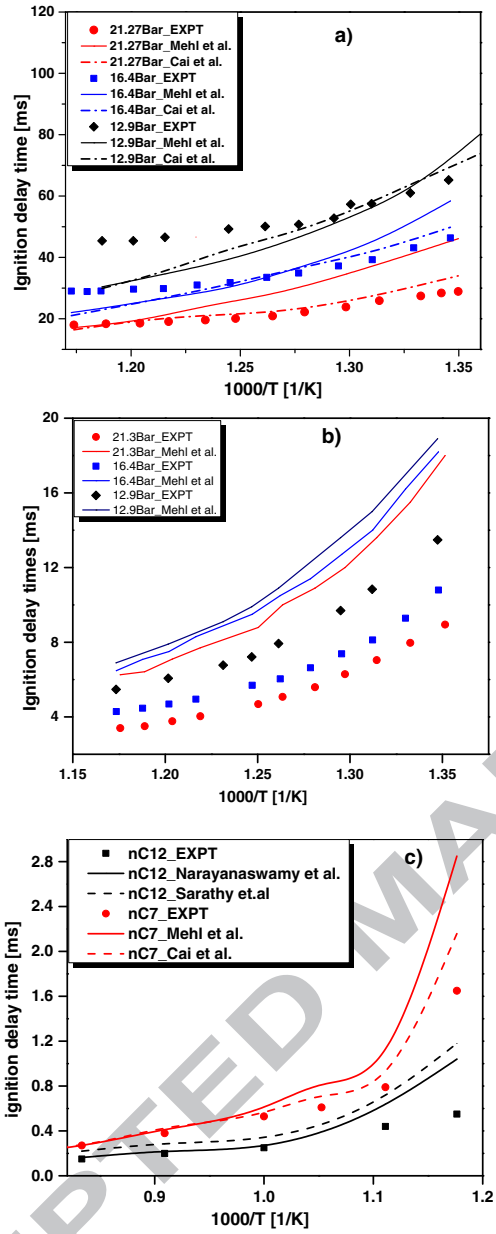

Figure 2. Simulated ignition delay times using various kinetic models compared against experimental a) iso-octane IQT data (this study), b) n-heptane IQT data (this study), and c) n-heptane [20] and n-dodecane CVCC data [20]

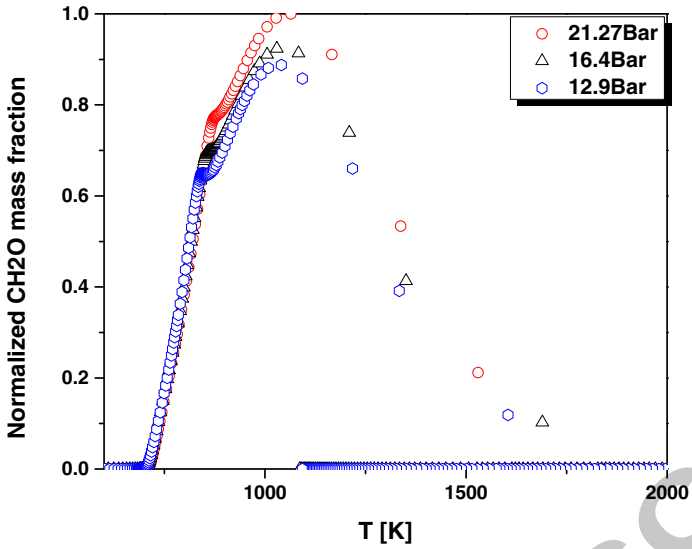

Figure 3. Normalized CH_2O mass fractions vs T [K] at different ambient pressures

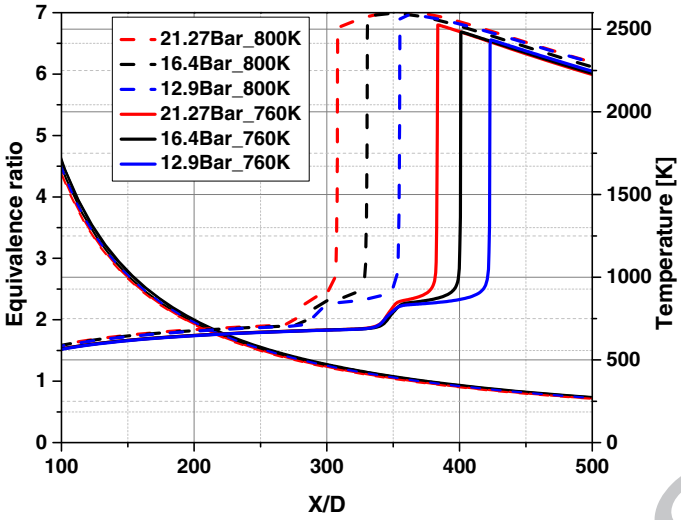

Figure 4. Variation in ignition location and corresponding equivalence ratios at different initial ambient temperatures and pressures

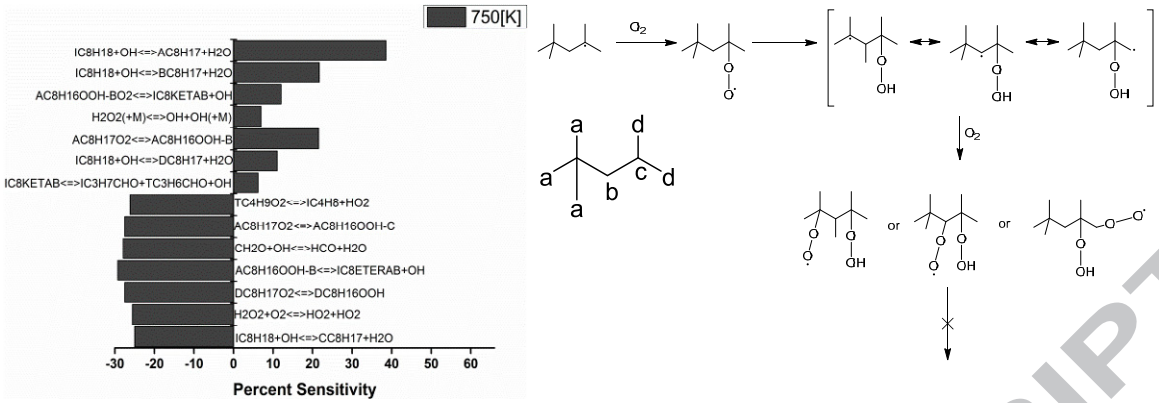

Fig. 5. a) Percentage sensitivity analyses to changes in reaction rate coefficients at ignition. Initial conditions for simulations: 21.27 bar, 750 K. b) Scheme of H-abstraction from *c*-position in *iso*-octane fuel

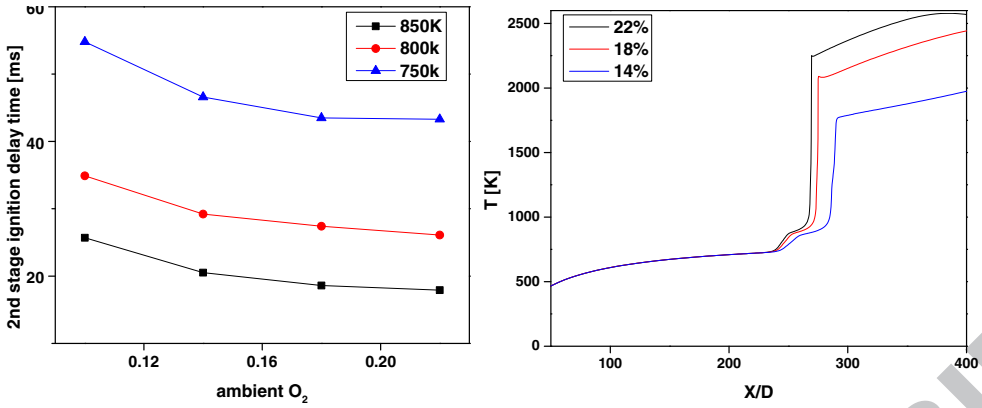

(a) (b)

Figure 6. Simulated effects of oxygen concentrations on a) second stage ignition delay time b) ignition location at 850 K

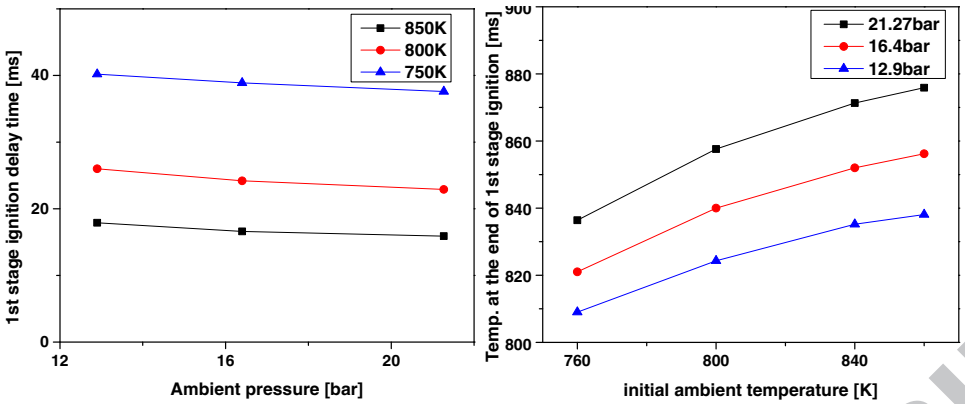

(a) (b)

Figure 7. Simulated effect of ambient pressure on a) first stage ignition delay time b) temperature at the end of the first stage ignition.

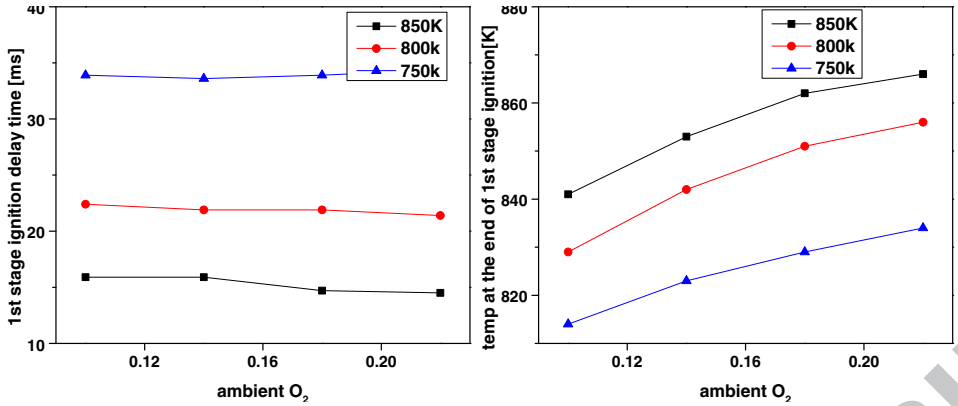

(a) (b)

Figure 8. Simulated effect of ambient oxygen concentration on a) first stage ignition delay time b) temperature at the end of the first stage ignition

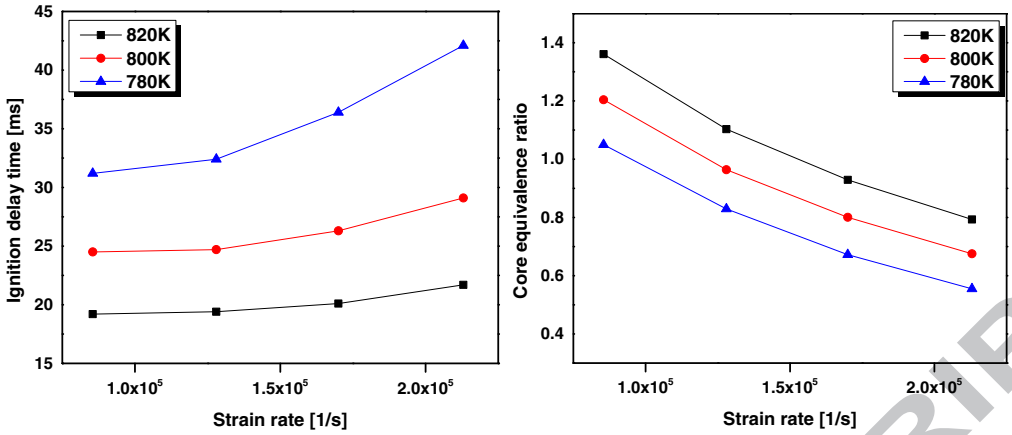

(a) (b)

Figure 9. Simulated effect of strain rate on a) second stage ignition delay time b) equivalence ratio at ignition

Table 1. Details adopted for TSL simulation

Mechanism	
LLNL Gasoline Surrogates	Mehl et al. (2009)
RWTH Gasoline Surrogates	Cai et. al.(2014)
C7-C20 2-methylalkanes	Sarathy et al. (2011)
n-Dodecane mechanism	Narayanaswamy et al. (2013)
Ambient gas	
IQT	Air
CVCC	O_2, CO_2, N_2
Pressure (bar)	
IQT	21.3, 16.4, 12.9
CVCC	49.3-50.6(*n*-heptane), 49.3-79.4(*n*-dodecane)
Temperature (K)	
IQT	720-860
CVCC	850-1200
Nozzle diameter(mm)	
IQT	0.722
CVCC	0.084
Temp. of the liquid fuel (K)	
IQT	326
CVCC	373
Injection Pressure (bar)	
IQT	179.26
CVCC	~1500
Injection duration (ms)	
IQT	2
CVCC	1.5
Fuel density (kg/m^3)	*n*-heptane(684), *iso*-octane(692), *n*-dodecane(752)

Highlights

- TSL model was used to simulate ignition delay time in the IQT and in the CVCC.
- TSL model is efficient in simulating IQT of long ignition delay time fuels and CVCC experiments.
- TSL modeling approach demonstrates the suitability of using detailed kinetic models to provide insights into spray combustion.